Subject	Chemistry
Paper No and Title	Paper 5: Organic Chemistry-II (Reaction Mechanism-I)
Module No and Title	Module 1: Types of Organic Reactions
Module Tag	CHE_P5_M1_e-Text

Principal Investigator		Co- Principal Investigator and Technical Coordinator
Prof A.K.Bakhshi Sir Shankar Lal Professor, Department of Chemistry University of Delhi		**Dr Vimal Rarh** Deputy Director, Centre for e-Learning and Assistant Professor, Department of Chemistry, SGTB Khalsa College, University of Delhi *Specialised in : e-Learning and Educational Technologies*
Paper Coordinator	**Content Writer**	**Reviewer**
Prof. Diwan S Rawat Department of Chemistry University of Delhi	**Prof. Diwan S Rawat** Professor Department of Chemistry University of Delhi **Dr. Beena Negi** Assistant Professor Department of Chemistry University of Delhi	**Prof. Kamal K. Kapoor** Department of Chemistry University of Jammu
Anchor Institute : SGTB Khalsa College, University of Delhi		

TABLE OF CONTENTS

1. Learning Outcomes

After studying this module, you shall be able to

- Know the various types of organic reactions
- Learn the difference between each type of reaction
- Identify the reaction types depending upon reactants and conditions
- Analyze organic reactions

2. Introduction

An organic reaction is a change in structure or functional group leading to formation of a new substance. The compound undergoing a change in structure or functional group is called a reactant or substrate. The knowledge of organic reactions helps in the synthesis of useful chemical compounds such as polymers, dyes, drugs, perfumes, cosmetics, fertilizers, food preservatives.

3. Types of Organic Reactions

The organic reactions can be generally classified as substitution, addition, elimination, rearrangement, oxidation and reduction reactions.

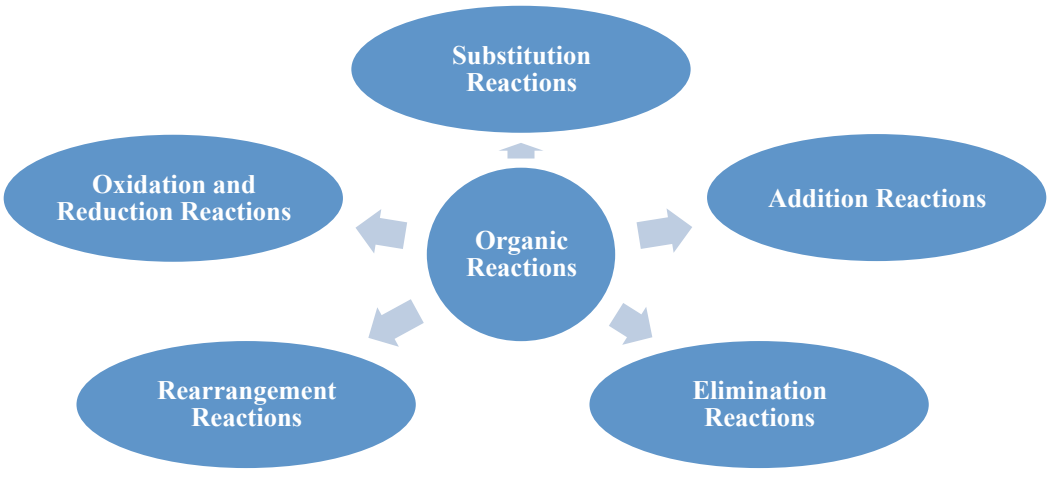

Fig 1: Types of organic reactions

3.1 Substitution Reactions

These reactions involve the displacement of an atom or a group by another atom or group.

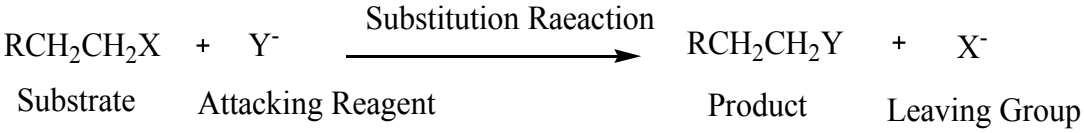

It takes place at
a) sp^3 hybridised carbon (alkane, haloalkane, alcohol)
b) sp^2 hybridised carbon (benzene)

A substitution reaction can be nucleophilic, electrophilic or free radical substitution reaction.

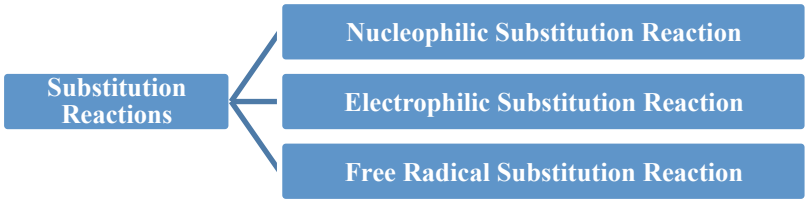

Fig 2: Types of substitution reactions

3.1.1 Nucleophilic Substitution Reactions

Attack of nucleophile at a saturated carbon atom, bearing a substituent known as leaving group results in a nucleophilic substitution reaction. The compound on which substitution takes place is called the substrate and the group that is displaced from carbon is called leaving group.

The nucleophilic reaction may follow the following pathways:

(a) Substitution nucleophilic unimolecular mechanism (S_N1)

Such reactions proceed in two steps *via* formation of a carbocation intermediate and the product obtained is a racemic mixture. For example, the hydrolysis of tertiary halides follow S_N1 pathway. The initiation step is ionization of substrate which is slow and rate determining step. The second step is a rapid reaction between the intermediate carbocation and the nucleophile.

Rate = k [RX]

Step 1 $R-X \underset{}{\overset{slow}{\rightleftharpoons}} R^+ + X$

Step 2 $R^+ + Y \xrightarrow{fast} R-Y$

(b) Substitution nucleophilic bimolecular mechanism (S_N2)

Such reactions proceed in one step *via* a transition state and inversion of configuration. For example, the hydrolysis of primary halides follow S_N2 pathway. In this mechanism, there is backside attack, the nucleophile approaches the substate from the position 180° away from the leaving group. This is a one step process with no intermediate.

Rate = k [RX] [Nu]

1

(c) Substitution nucleophilic internal mechanism (S_Ni)

In the reaction of alcohol with thionyl chloride, displacement of hydroxyl group by chloride proceeds *via* S_Ni mechanism. In this reaction the configuration is retained and it follows second order kinetics. In S_Ni mechanism, part of the leaving group must be able to attack the substrate, detaching itself from the rest of the leaving group in the process.

Rate = k [ROH] [$SOCl_2$]

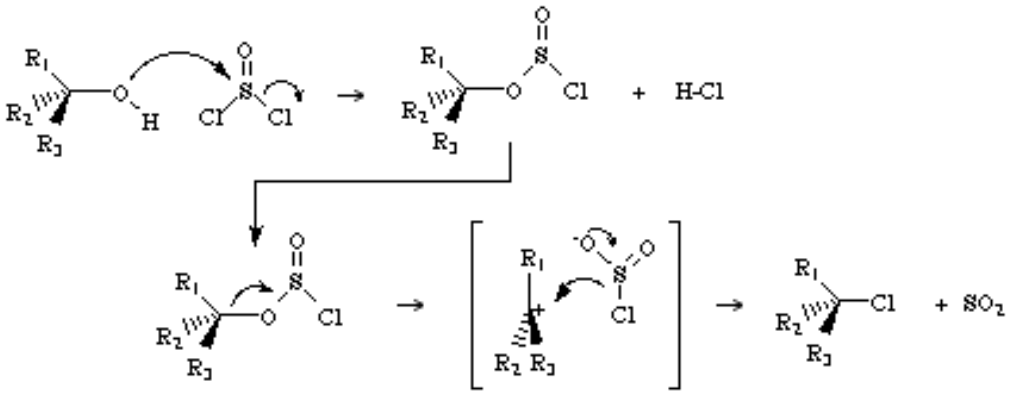

(d) Aromatic nucleophilic substitution (S_NAr)

In nucleophilic aromatic substitution a strong nucleophile replace a leaving group. The initiation step is usually, but not always, rate-determining. In general, the attacking species forms a bond with the substrate, giving an intermediate and then the leaving group departs.

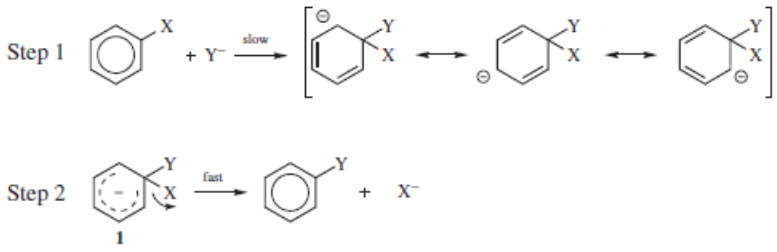

3.1.2 Electrophilic Substitution Reactions

It involves substitution in the aromatic ring by an electrophile. In the first step the electrophile is attacked by the π-electrons of the aromatic ring leading to the formation of a new carbon-electrophile bond. It is followed by loss of a proton. In these reaction, electrophile first attack to give an intermediate with positive charge, known as arenium ion and in the second step leaving group departs. This is known as arenium ion mechanism.

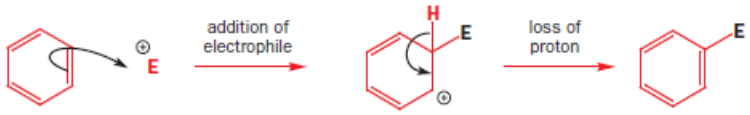

Examples of electrophilic substitution reactions are:
(a) Nitration: It involves a nitronium ion (NO_2) as an electrophile.

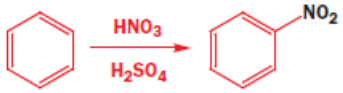

(b) Sulphonation: In this reaction sulphur trioxide (SO_3) acts as an electrophile.

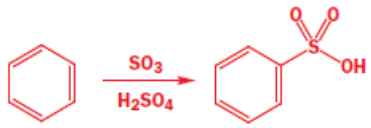

benzenesulfonic acid

3.1.3 Free Radical Substitution Reactions

Such reactions begin with the formation of a free radical which substitutes a group or atom present in the reactant molecule. The reaction of methane with chlorine in the presence of light is a free radical substitution reaction.

$$\mathbf{CH_4 + Cl_2 \longrightarrow CH_3Cl + HCl}$$

The first step is initiation i.e free radical formation by homolytic cleavage of bonds. Second step is chain propagation and finally chain termination step

Initiation

Initiation step may happen spontaneously or may be induced by heat or light depending on the type of bond.

$$Cl_2 \longrightarrow 2Cl\bullet$$

Chain Propagation

In this step, a molecule reacts with a free radical to generate a new radical.

$$CH_4 + Cl\bullet \longrightarrow CH_3\bullet + HCl$$

$$CH_3\bullet + Cl_2 \longrightarrow CH_3Cl + Cl\bullet$$

Chain termination

This step is also known as destruction of free radicals. This step involves a combination of two like or unlike radicals to form a new bond.

$$2Cl\bullet \longrightarrow Cl_2$$

$$CH_3\bullet + Cl\bullet \longrightarrow CH_3Cl$$

$$CH_3\bullet + CH_3\bullet \longrightarrow CH_3CH_3$$

3.2 Addition Reactions

These reactions are characteristic of compounds containing multiple bonds. The alkene (=), alkynes (≡), C=O, C≡N react by addition to multiple bond. Thus in addition reaction there is increase in the number of groups attached to the substrate and decrease in its unsaturation.

Addition reactions are of four type namely electrophilic, nucleophilic, free radical and concerted. The first three are the two-step processes, with initial attack by electrophile, nucleophile or a free

radical. The second step consists of a combination of the resulting intermediate with a negative species, a positive species or a neutral entity. In addition, attack at the two carbon atoms of the double or triple bond is simultaneous.

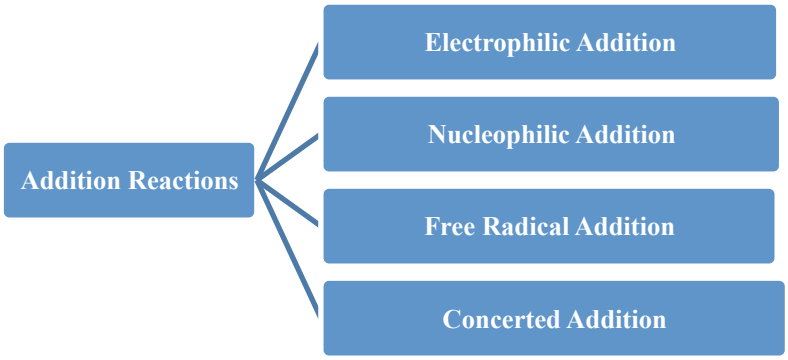

Fig 3: Types of addition reactions

3.2.1 Electrophilic Addition Reactions

The first step is addition of electrophile by formation of σ bond through donation of π electrons to the electrophile and carbocation is formed. The next step is reaction of the positively charged intermediate (carbocation) with a species carrying lone pair or negative charge i.e nucleophiles. This step is the same as the second step of the S_N1 mechanism.

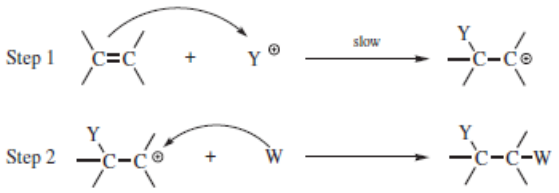

Examples of electrophilic addition reactions:

(a) Addition of bromine to alkenes: The addition reaction of bromine to alkenes proceeds via a cyclic bromonium ion intermediate. This intermediate is similar to those encountered in the neighbouring-group mechanism of nucleophilic substitution. This reaction is used as a colour test to detect the presence of multiple bonds. The brown colour of bromine disappears when it is added to a compound with double or triple bonds.

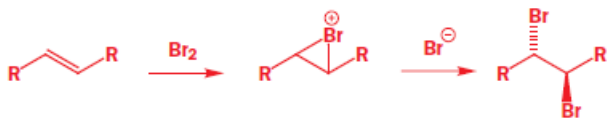

(b) Addition of unsymmetrical reagents to unsymmetrical alkenes (Markownikoff rule): For example in the reaction of propene with HBr, H^+ acts as an electrophile which is added to the carbon bearing double bond followed by attack of bromide ion (Br^-).

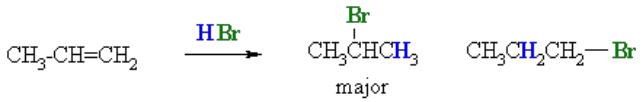

3.2.2 Nucleophilic Addition Reactions

Such reactions are encountered in compounds containing polar functional groups (C=O, C≡N, C=S). In the first step a nucleophile with its pair of electrons attacks the carbon atom of a double or triple bond, forming a carbanion. It is followed by a second step in which this carbanion reacts with a positive species.

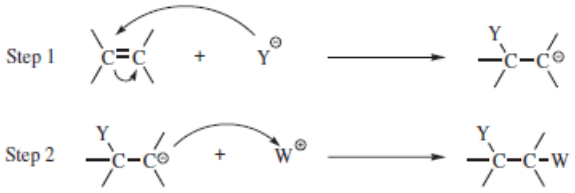

When the olefin contains a good leaving group (as defined for nuclepohilic substitution), substitution is a side reaction.(i.e. a nucleophilic substitution at a vinylic substrate).

Examples of nucleophilic addition reactions:

(a) Addition of HCN to carbonyl group: In this reaction cyanide ion (CN^-) acts as a nucleophile which attacks the carbon of carbonyl group, the carbon-oxygen double bond breaks followed by capture of proton and a cyanohydrins is formed.

(b)Addition of alcohol to carbonyl compounds: Aldehydes or ketone react with one mole of alcohol to form hemiacetal or hemiketal, respectively. Reaction with second mole of alcohol gives acetal or ketal. In this reaction the alcohol with lone pair of electrons of oxygen atom acts as a nucleophile

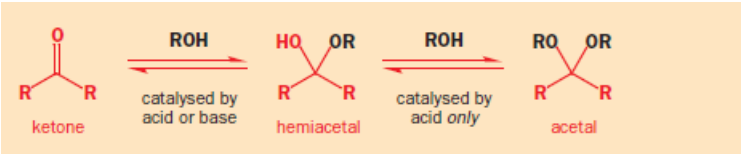

(c) Nucleophilic addition to carbon-carbon double bond (Michael reaction): In Michael reaction a nucleophile adds on to the β-carbon of an α,β-unsaturated system having electron withdrawing group. HY added to substrate having groups such as CHO, COR, COOR, $CONH_2$, CN,NO_2, SOR,SOOR etc. always give a product with Y^- bonding with the carbon away from the Z group and follows nucleophilic mechanism.

CH_2=CH-CN + H-Y ---------→ Y-CH_2-CH_2-CN

This 1,4- addition is called as cyanoethylation because Y is cyanoethylated.

3.2.3 Free Radical Addition Reactions

Free radicals add to an unsaturated molecule to give a new radical intermediate which further reacts to give final product. The radical is generated by photolight or spontaneous dissociation.

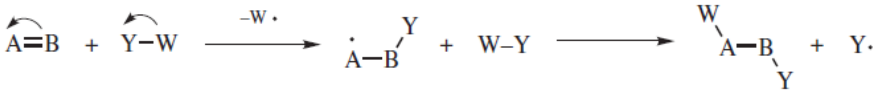

Example of free radical addition reaction:

Addition of HBr to alkene in presence of peroxide (Anti-Markownikoff addition) is a type of free radical addition reaction. The peroxide acts as radical initiator. This is a stereoselective free-radical addition reaction.

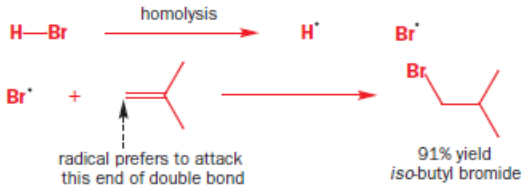

3.2.4. Concerted Addition Reactions

Concerted addition reactions occur by simultaneous attack at both the carbons. The initial attack is not at one carbon of the double bond, but both carbons are attacked simultaneously. Most of these reactions involve four-membered transition state but in few cases, there is a five- or six-membered transition state. In these cases, the addition to the double or triple bond must be *syn*. The most important reaction of this type is Diels-Alder reaction.

Example of concerted addition reaction:

Hydroboration of alkene is a concerted addition reaction. Here, the formation of C-H and C-B bonds takes place at the same time of breaking of the B-H bond.

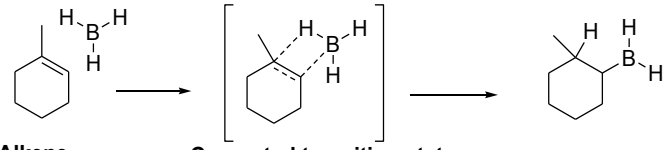

3.3 Elimination Reactions

In these reactions two atoms or groups attached to the carbon atom/s of the substrate molecule are eliminated. These are of three types α, β and γ eliminations.

α-elimination (or 1,1- elimination): The two groups are eliminated from same carbon, for example formation of carbene or nitrene.

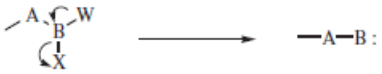

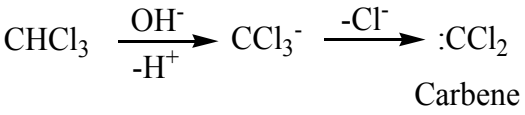

β-elimination (or 1,2-elimination): This is the most common elimination reaction in which the two groups are eliminated from adjacent carbons creating a multiple bond. In most β-eliminations, the new bonds are c=c or c≡c. The β-eliminations include acid catalysed dehydration of alcohols, Hofmann elimination, dehydrohalogenation.

γ-elimination: A three membered ring is formed in this case.

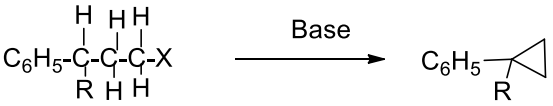

R = H or C_6H_5
X = F or OTs

The β-elimination reactions follow two pathways E1 and E2.

3.3.1 Unimolecular Elimination Mechanism (E1)

The E1 reaction needs no good base or nucleophile, it proceeds via formation of a carbocation. It is a two-step reaction involving formation of a carbocation followed by loss of proton giving more substituted alkene as major product. Here, formation of carbocation by ionization of substrate is the rate determining step. The carbocation so formed rapidly loses a β proton to a base, usually the solvent. E1 is analogous to S_N1 mechanism. The second step differs in that the solvent pulls a proton from the β carbon of a carbocation rather than attacking it at the positively charged carbon, as in the S_N1 process. In E1 reaction, the product should be completely non-stereospecific, since the carbocation is free to adopt its most stable conformation before losing proton.

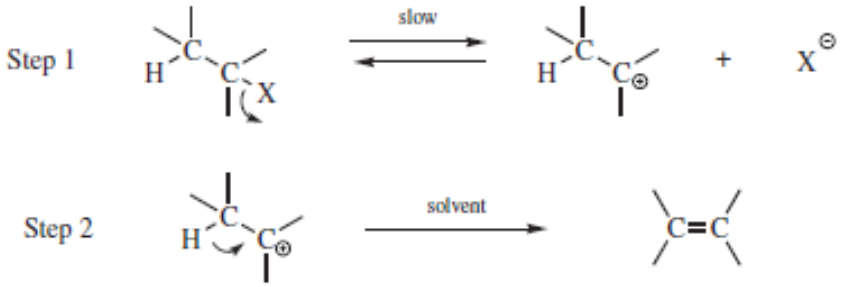

3.3.2 Bimolecular Elimination Mechanism (E2)

In E2 mechanism a strong base abstracts proton from the substrate and the electron pair form π-bond with departure of leaving group, all this occurs in one step. The two groups are eliminated simultaneously. It occurs in one step thus follows second order kinetics *i.e.*first order in substrate and first order in base. E2 is analogous to the S_N2 mechanism and often competes with it. Dehydrohalogenation of alkyl halides to alkene is a bimolecular elimination reaction.

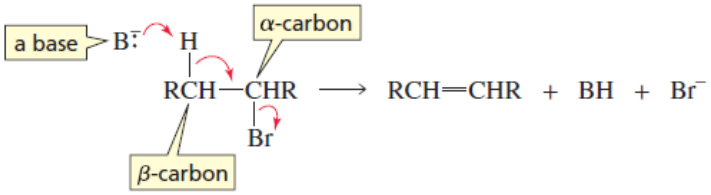

3.4. Rearrangement Reactions

Molecular rearrangements involve migration of an atom or a group from one atom to another in the same molecule. The rearrangement reactions proceed via the formation of cation, anion or radical. The 1,2-rearrangement, pericyclic reactions and metathesis occur via rearrangement. The atom A is called Migration Origin and B is the Migration terminus. The migration of any substituent from one atom to the atom adjacent to it is known as 1,2- shifts, but some are over longer distances.

Examples of rearrangement reactions:

(a) Pinacol-Pinacolone rearrangement: Conversion of 2,3-dimethylbutan-2,3-diol into 2,2-dimethylbutan-3-one.

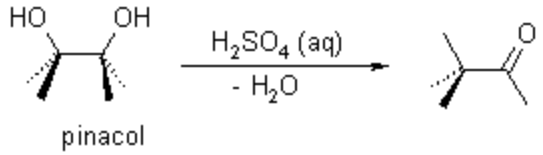

(b) Beckmann rearrangement: Conversion of an oxime to amide is a rearrangement reaction. In most Beckmann rearrangements, only the groups trans (usually called anti) to the hydroxyl group migrates.

(c) Pericyclic Reactions: A pericyclic reaction involves concerted bond reorganisation and the essential bonding changes within a cyclic array of the participating atomic centres. In these types of reaction neither ions nor radicals are formed as intermediate and remain unaffected by polar reagents. They take place either photochemically or thermally.

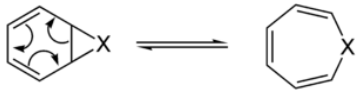

X = CR_2, NR, O

3.5 Oxidation and Reduction Reactions

Organic reactions are classified as oxidation or reduction depending on whether the substrate is oxidised or reduced. For this the functional groups are arranged in order of increasing oxidation state as follows:

Oxidation state -4 (alkane)
Oxidation state -2 (alkene, alcohol, alkyl halide, amine)
Oxidation state 0 (alkyne, carbonyl, dihalides, diols)
Oxidation state +2 (carboxylic acid, amide, trihalide)
Oxidation state +4 (carbon dioxide, carbon tetrachloride)

Oxidation is the conversion of a functional group in a molecule from one category to a higher one and reduction is the opposite. In oxidation gain of oxygen or/and loss of hydrogen takes place. Reduction is opposite to that of oxidation as here loss of oxygen or gain of hydrogen takes place. Also there is no oxidation without a concurrent reduction.

Oxidation reactions are classified depending on the type of bond change involved.

Examples of oxidation reactions:

Elimination of hydrogen.

(a) Aromatisation: Conversion of cyclohexane to benzene in the presence of a catalyst is a type of oxidation reaction which proceeds via loss of hydrogen. The most frequently used reagents to affect aromatization are hydrogenation catalysts such as Pt, Pd, Ni etc. quinines, elements S, Se etc.

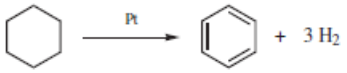

(b) Oxidation or dehydrogenation of alcohols to aldehydes and ketones. Conversion of alcohol to carbonyl: A variety of reagents such as CrO3, pyridinium chlorochromate (PCC), pyridinium dichromate (PDC), DMSO/oxalyl chloride, DMSO/DCC, copper chromite, are used for oxidation of alcohols to aldehyde or ketone. Primary alcohols are converted to aldehydes and secondary alcohols are converted to ketones in four main ways:

1). With strong oxidizing agents .

2). By catalytic dehydrogenation.

3). With NBS and other chemoselective oxidising agents.

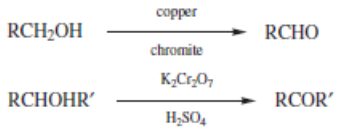

(c) Cleavage of carbon- carbon bonds *i.e.* Ozonolysis: Reaction of alkenes with ozone under suitable conditions leads to fission of carbon-carbon double bond via formation of an intermediate ozonide.

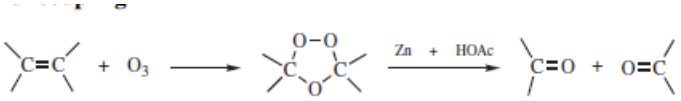

16

Examples of reduction reaction:

(a) Conversion of carbonyl to alcohol: When aldehydes or ketones are converted to alcohol the hydrogen content is increased thus it is a reduction reaction. The transfer of hydride ion by lithium hydride to carbonyl is such an example. There are two methods known for the conversion of carbonyl to alcohol, these are Clemmensen reduction and the wolff kishner reduction.

(b) Meerwein–Ponndorf–Verley reduction: It occurs in the presence of isopropyl alcohol and aluminum isopropoxide. The reaction is reversible in nature and the reaction reverse to it is named as the Oppenauer oxidation.

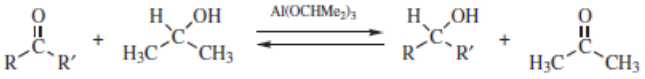

(c) Clemensen Reduction: In the Clemensen reduction a carbonyl compound is reduced to alkane using amalgamated zinc and hydrochloric acid. Ketones are reduced more often than aldehydes.

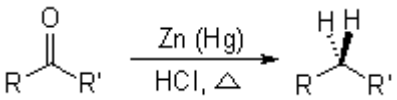

(d) Conversion of carboxylic ester to alcohol: Lithium hydride often brings out reduction of carboxylic ester by hydride transfer via formation of aldehyde in first step and further hydride transfer to the aldehyde leads to formation of alcohol. This reaction is of wide scope and has been used to reduce many esters. Other common reagents used are DIBAL, Lithium triethylborohydride, BH_3-SMe_2 in refluxing THF. $NaBH_4$ reduces phenolic esters especially those containing EWGs.

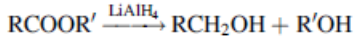

(e) Conversion of nitro compounds to amine: Conversion of nitro group to amine is a reduction reaction which involves loss of oxygen and gain of hydrogen.

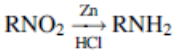

Both aliphatic and aromatic nitro compounds can be reduced to amines, though the reaction has been applied much more often to aromatic nitro compounds. The other common reagents are Zn, Sn or/and acid, AlH_3-$AlCl_3$, $TiCl_3$, Al-$NiCl_2$-THF, formic acid and Pd-C, etc.

4. Summary

- Organic reactions are of various types.
- Organic reactions are classified as substitution, addition, elimination, rearrangement, oxidation and reduction.
- These reactions differ mechanistically from each other and on the nature of attacking reagents.

Subject	Chemistry
Paper No and Title	Paper No. 5:Organic Chemistry-II
Module No and Title	Module No. 2: Overview of different types of Organic Reaction Mechanisms
Module Tag	CHE_P5_M2

Principal Investigator		Co- Principal Investigator and Technical Coordinator
Prof A.K.Bakhshi Sir Shankar Lal Professor, Department of Chemistry University of Delhi		**Dr Vimal Rarh** Deputy Director, Centre for e-Learning and Assistant Professor, Department of Chemistry, SGTB Khalsa College, University of Delhi *Specialised in : e-Learning and Educational Technologies*
Paper Coordinator	**Content Writer**	**Reviewer**
Prof. Diwan S Rawat Department of Chemistry University of Delhi	**Prof. Diwan S Rawat** Professor Department of Chemistry University of Delhi **Dr. Beena Negi** Assistant Professor Department of Chemistry University of Delhi	**Prof. Kamal K. Kapoor** Department of Chemistry University of Jammu
Anchor Institute : SGTB Khalsa College, University of Delhi		

TABLE OF CONTENTS

1. Learning Outcomes

After studying this module, you shall be able to:

- Know how organic reactions proceed.
- Identify the different types of reaction mechanisms.
- Analyse the difference between each type of mechanism.

2. Introduction

Reaction Mechanism: Mechanism for any reaction is defined as collection of number of processes that explains the overall reaction.

- This is the actual method of completion of reaction as it gives the number of broken bonds and the number of steps involved.
- In a mechanism thepositions of all atoms (stereochemistry), role of solvent molecules and the energy of thesystem is specified.
- It also helps in describing the reaction intermediate, activated complex and transition state involved in the whole reaction.
- A mechanism accounts for all the reactants used, the function of a catalyst, all products formed and their amount.
- From a mechanism the rate law can be deduced.

You are already familiar with some common terms frequently encountered while discussing any reaction mechanism as given below:

Substrate: In most reactions of organic compounds, one or more covalent bonds are broken.For most reactions, it is convenient to call one reactant the attacking reagent and the other the substrate.

Nucleophile and Electrophile: Reagent having an electron pair is known as nucleophile and the reaction is nucleophilic. A reagent that takes an electron pair is called an electrophile and the reaction is electrophilic.

Leaving Group: In a reaction in which the substrate molecule becomes cleaved, part ofit (the part not containing the carbon) is usually called the leaving group. A leaving group that carries away an electron pair is called a nucleofuge. If itcomes away without the electron pair, it is called an electrofuge.

Reaction intermediates: Intermediates are those chemical species which are short-lived and unstable. They are neither reactant nor product. They are said to be temporary products or reactants generally free radicals or ions.
Transition states: It is an unstable intermediate molecular state with an unusual number of bonds and/or unstable geometry.

Molecularity: It is defined as number of colliding molecular entities involved in a single reaction step.

- Unimolecular reaction step involve only one molecular entity.
- Bimolecular reaction step involve two molecular entities.
- Termolecular reaction step involve three molecular entities.

3. Types of Reaction Mechanisms

Organic reactions proceeds via various mechanisms some common mechanisms are S_N1, S_N2, S_Ni, S_NAr (addition-elimination, elimination-addition, aryl cation), SR_N1, EAS, E1,E2,E1cb,Ei,free radical mechanism and concerted mechanism.

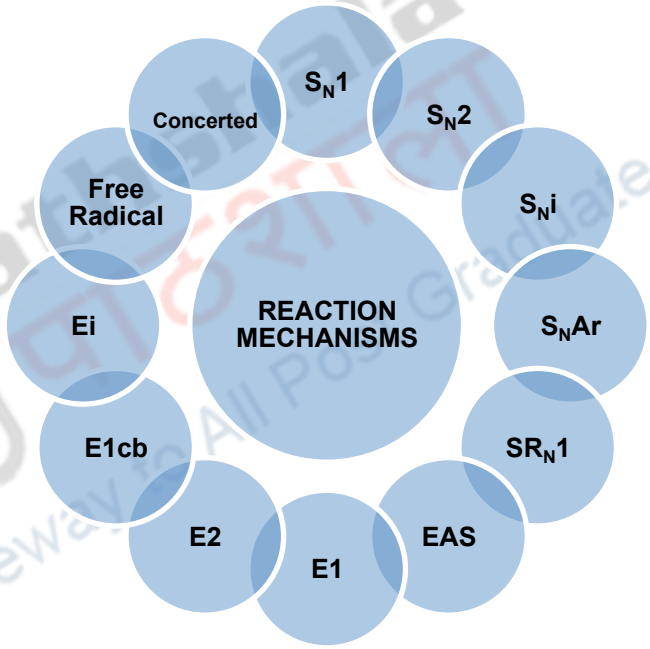

Figure 1: Types of reaction mechanisms

3.1.Substitution Nucleophilic Unimolecular Mechanism (S_N1)

The reaction between tert alkyl halides (eg. *tert*-butylbromide) and water followsSubstitution NucleophilicUnimolecular Mechanism (S_N1).Unimolecular means that only one molecule is involved in the rate-determining step.

The mechanism of S_N1 reaction is as follows:

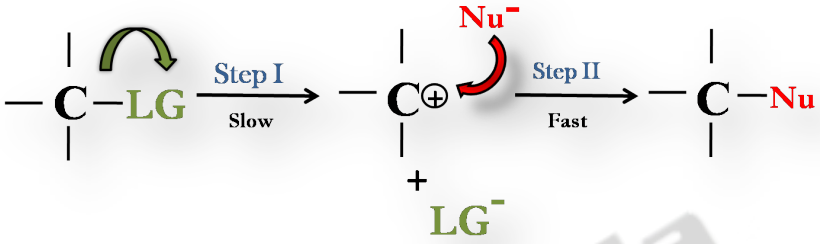

- S_N1 reaction proceeds in two steps.
- Step 1 is formation of carbocation.
- Step 2 is capture of carbocation by nucleophile.
- Follow first order kinetics. Because, the rate of the reaction depends on the concentration of only one reactant i.e. alkyl halide in this case, the reaction is a first-order reaction.
- Rate law is define as:

Rate = k [RX]

- Two stereoisomers are formed for an alkyl halide having asymmetric carbon.Oneof the products has the same relative configuration at the asymmetric carbon as the reacting alkyl halide while the other has inverted configuration..
- The order of reactivity for alkyl halides is $3^o > 2^o > 1^o > CH_3X$
- As reaction proceeds through formation of carbocation there is possibility of rearrangement to form more stable carbocation.
- S_N1 is favoured in polar protic solvent and in the presence of weak nucleophile.

3.2 Substitution Nucleophilic Bimolecular Mechanism (S_N2)

The reaction of methyl bromide with hydroxide ion follows S_N2 mechanism.When the transition state is reached, the central carbon atom has gone from its initial sp^3 hybridisation to a sp^2 state with an approximately perpendicular p orbital. There are two lobes of p-orbital, one overlaps with the leaving group and the other with nucleophile. During transition state the three non-reacting substituents and the central carbon are in a same plane. This inversion of configuration is called Walden inversion.

The mechanism of S_N2 reaction is as follows:

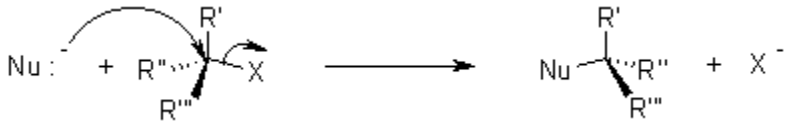

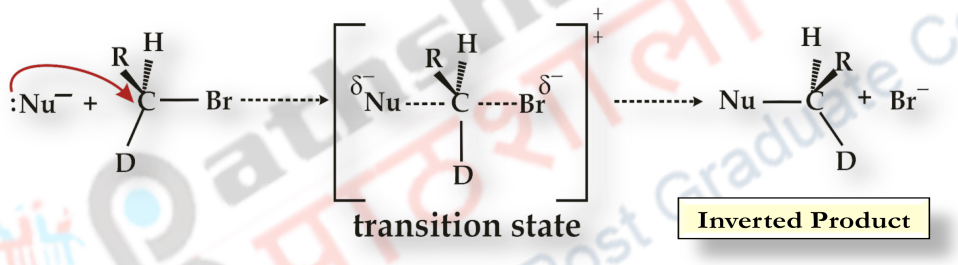

- An alkyl halide having an asymmetric carbon results in the formation of only one stereoisomer and the inversion of configuration takes place.

- Reactions following S_N2 mechanism occur in one step via formation of a transition state.

- The rate of the nucleophilic substitution depends upon the concentration of reactant, methyl bromide in this case,if the concentration of reactant doubles, the rate of the nucleophilic substitution reaction also doubles.
- The rate of the reaction also depends on nucleophile concentration. This means that both reactants are involved in the rate determining step.

  Hence the rate law is:

  Rate = k [RX] [Nu]

- Polar aprotic solvents favour S_N2.

3.3 Substitution Nucleophilic Internal Mechanism (S_Ni)

Replacement of OH of alcohols by Cl in the presence of $SOCl_2$ proceeds via S_Ni mechanism. It follow second order rate law. This reaction proceeds with the retention of configuration.

Rate = k [ROH] [$SOCl_2$]

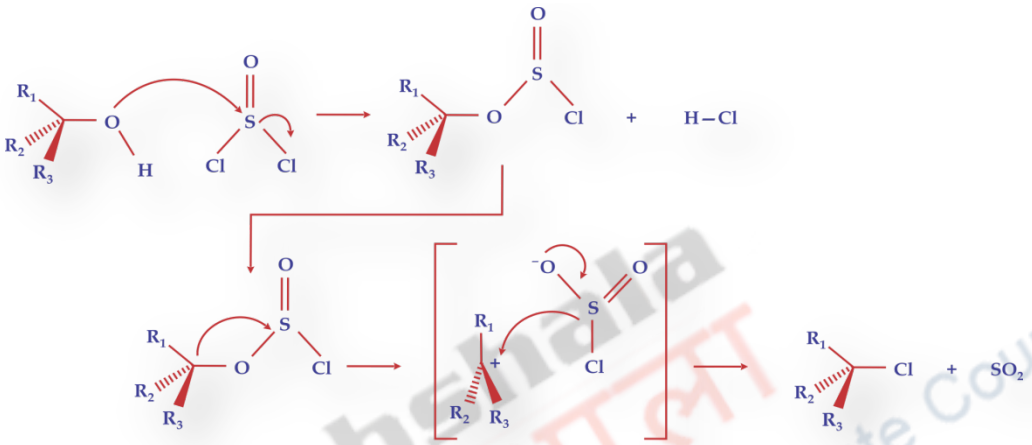

3.4 Aromatic Nucleophilic Substitution Mechanism (S_NAr)

In aromatic nucleophilic substitution mechanism a strong nucleophile replaces aleaving group. It can be through an addition-elimination, elimination-addition or aryl cation mechanism.

3.4.1 The S_NAr Addition-Elimination Mechanism

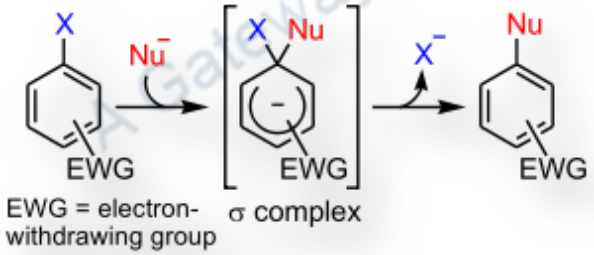

Here substitution takes place at ipso position. Presence of strong electron withdrawing group at ortho/para to leaving group favors addition-elimination mechanism. It uses one of the vacant π^* orbitals for bonding interaction with the nucleophile. This allows addition of nucleophile to the aromatic ring without displacing any substituent. Net substitution occurs in second step by elimination of leaving group.

Example of reaction undergoing through addition-elimination mechanism: Reaction of para-nitro fluoro benzene with sodium methoxide.

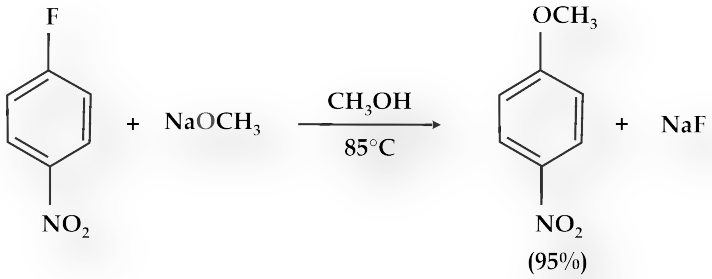

It is a two step mechanism and proceeds as shown:

(i) Slow step: Aromaticity of ring is lost in this step. Nucleophile attacks on bond between carbon and halogen.

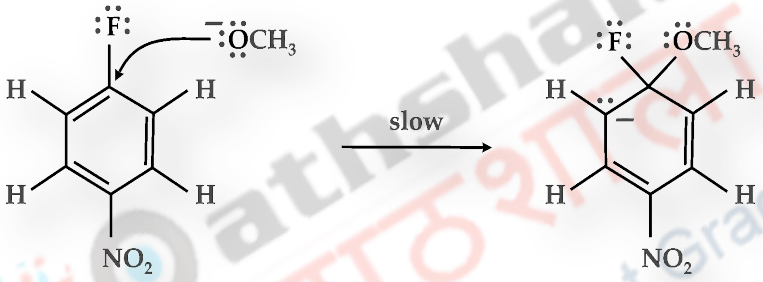

The intermediate formed is stabilised via resonance. Presence of electron withdrawing group at ortho or para position provides extra stabilisation.

(ii) Fast step: Aromaticity of the ring is restored in this step. Intermediate formed in first step looseshalide.

3.4.2 Elimination-Addition Mechanism (BenzyneMechanism)

Elimination-addition mechanism involves a highly unstable intermediate called dehydrobenzene or benzyne.

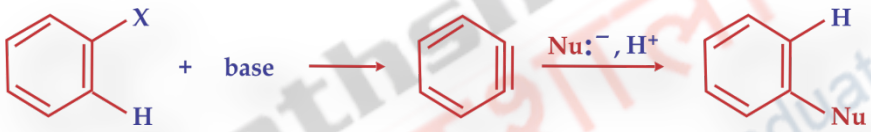

Example of elimination-addition mechanism: Reaction of chlorobenzene with soda amide in liquid ammonia. If the aryl halide contains two ortho substituents, the reaction should not occur.

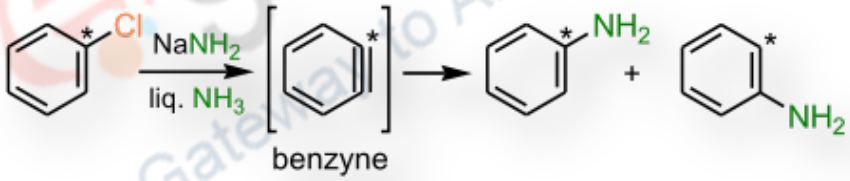

The mechanism of this reaction is shown below:
(i) First step is elimination of proton ortho to the substituent present and formation of benzyne.

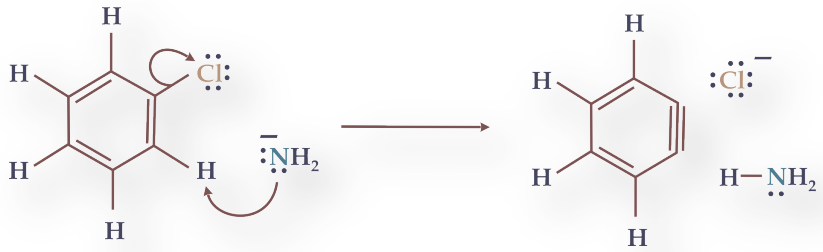

(ii) Attack of amide ion on the benzyne intermediate.

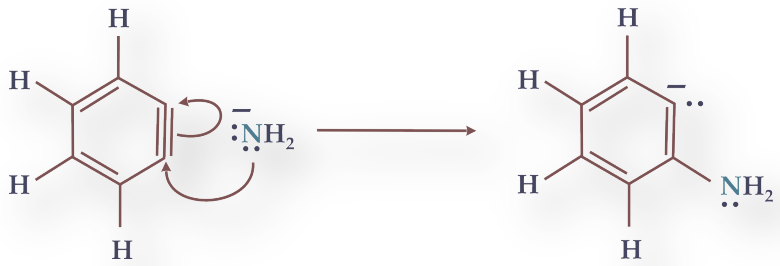

(iii) Abstraction of proton from ammonia.

3.4.2 Aryl Cation Mechanism

The aromatic aryl cation S_N1 mechanism is encountered with diazonium salts. The reaction rate is first order in diazonium salt and independent of the concentration of nucleophile.

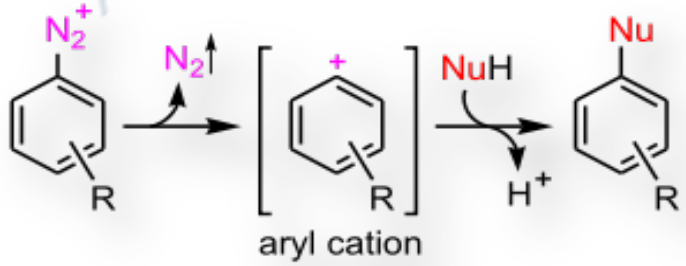

3.5 Substitution Radical Nucleophilic Unimolecular($S_{RN}1$)

This was discovered in 1970 by Bunnett and Kim where, $S_{RN}1$ stands for substitution radical-nucleophilic unimolecular as it is similar to aliphatic S_N1 reaction.
$S_{RN}1$ is a substitution reaction in which nucleophilic substitution on aromatic compound takes place.

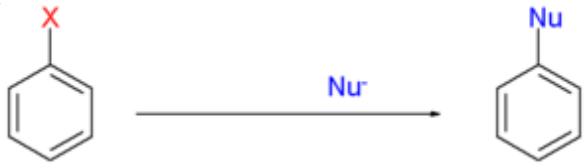

Where, X is a halide.

.

An example of this reaction type is the Sandmeyer reaction which involves synthesis of aryl halides from aryl diazonium salts via $S_{RN}1$ mechanism.

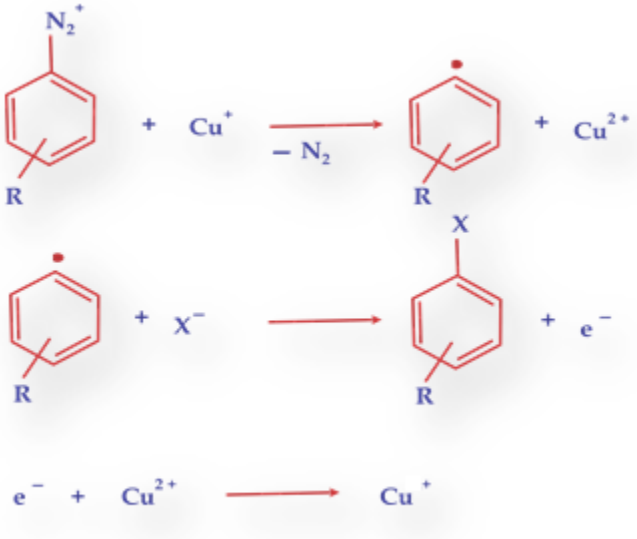

3.6 Electrophilic Aromatic Substitution Mechanism (EAS)

It involves attack of π-system on electrophile and the stabilization of benzenonium ion through resonance and removal of proton by base.

Examples of reactions undergoing EAS mechanism are nitration, sulphonation, halogenations, Friedel and Craft reactions. Ions formed in this mechanism are known as Wheland intermediates, σ complexes or arenium ions.

1. Generation of electrophile

2. Attack of electrophile on aromatic ring forming carbocation intermediate

3. Deprotonation

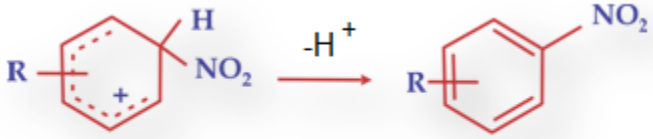

3.7Unimolecular Elimination Mechanism (E1)

First step of a Unimolecular Elimination Mechanism (E1) is the loss of leaving group and formation of a carbocation which is a slow and rate limiting step. The overall elimination is completed by rapid removal of proton from adjacent carbon by attack of base (B:) leading to formation of a double bond between the two carbon atoms.

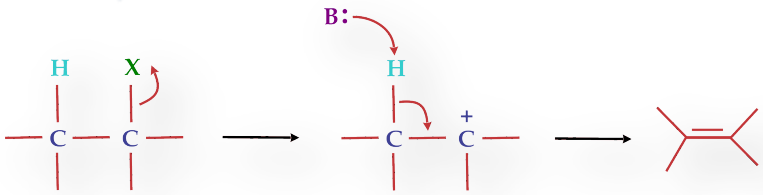

- Rate of elimination is dependent on the concentration of the substrate.
  i.e., Rate = k [RX].

- Reaction is independent of nucleophile.
- Reaction is first order.
- It is favoured by protic polar solvent.
- Rearrangement may take place.
- A strong base not required.
- A good leaving group is required, such as a halide or a tosylate.
- The mechanism goes through carbocation intermediate, therefore rearrangement can take place.

Example of Unimolecular Elimination Mechanism (E1): Dehydrohalogenation of alkyl halide.

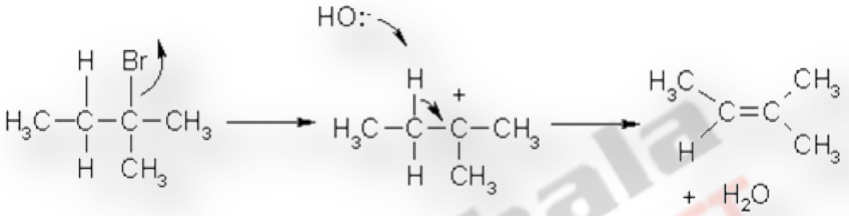

3.8Bimolecular Elimination Mechanism (E2)

In the Bimolecular Elimination Mechanism (E2), a base (B:) abstracts a proton from a carbon adjacent to the carbon attached to the leaving group. The electron pair left on the carbon force the leaving group to leave and create a double bond. All this occur simultaneously in this mechanism.

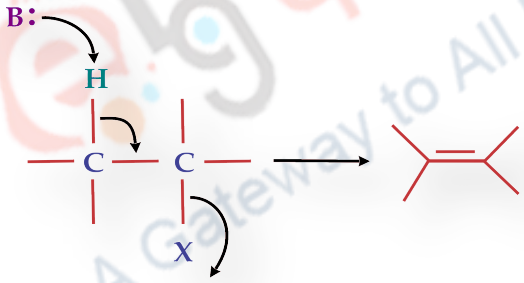

- E2 is a one step process. C-H and C-X bond breaking takes place simultaneously in one step.
- Rate of elimination depend on concentration of substrate and base. It follows second order kinetics.

  Rate = k [RX] [B]
- High concentration and strong base favours E2.
- It requires aprotic solvent.
- In E2 1,2-elimination takes place.

- A good leaving group is required, such as a halide or a tosylate.

Examples of Bimolecular Elimination Mechanism (E2):
(i) Acid catalysed dehydration of alcohols.
(ii) Hoffman degradation of quarternary ammonium hydroxides.
(iii) The base induced elimination of hydrogen halide from alkyl halide.

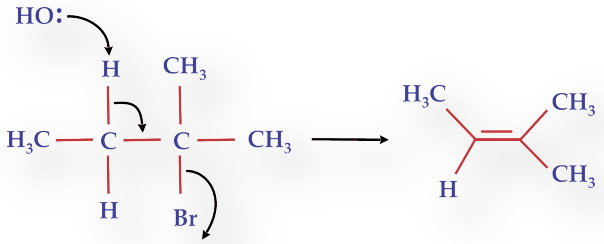

3.9 Conjugate Base Elimination Mechanism (E1cb)

In a Conjugate Base Elimination Mechanism (E1cb) the C-H bond breaks with formation of carbanion as intermediate. Formation of carbanion is fast and loss of leaving group is slow and rate limiting. The greatest likelihood of finding E1cb mechanism is in substrates that have a) poor nucleofuge b)an acidic hydrogen.

Rate = k [RX] [B]

The E1 mechanism requires formation of a primary carbocation,whereas the E1cb proceeds via a carbanion intermediate.

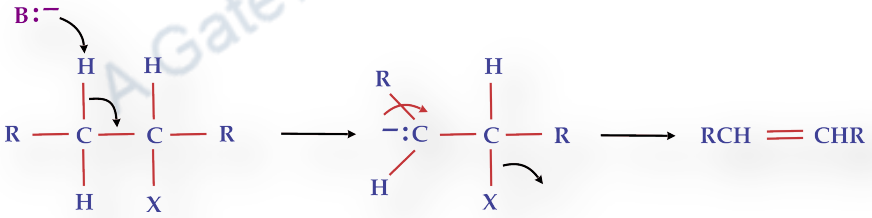

3.10 Elimination InternalMechanism (Ei)

In Elimination Internal mechanism (Ei), two vicinal substituents on an alkane framework leave simultaneously in a single step and formation of alkene takes place in a syn elimination.

Examples of Ei mechanism:

(a) The Burgess Reagent or methyl *N*-(triethylammoniumsulfonyl)carbamate is a dehydrating reagent mild in nature. it involves the conversion of secondary and tertiary alcohol to alkenes in a syn-elimination.

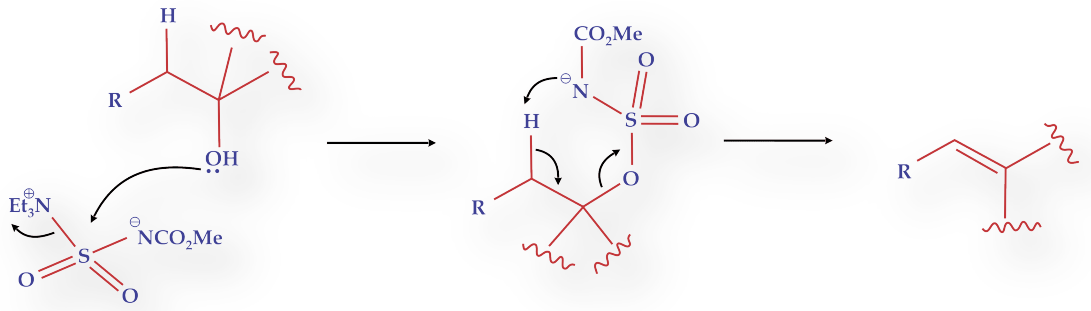

(b) The Cope reaction is an elimination reaction involved in the formation of 5-membered cyclic (intramolecular) transition state. In this reaction, alkene and a hydroxylamine is formed.

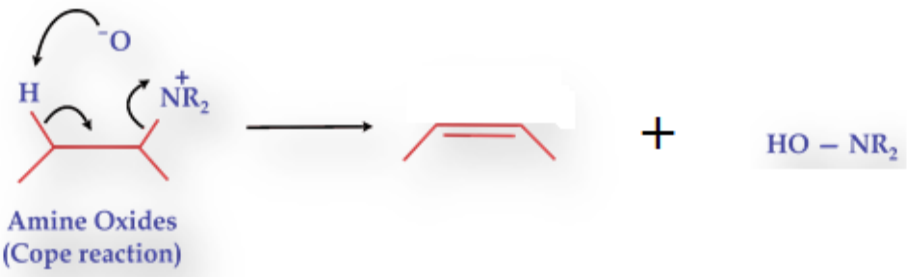

3.11 Free Radical Mechanism

In radical mechanism hemolytic bond cleavage takes place. The free radicals are involved in chain reaction which leads to chain propagation. The final step chain termination involves combination of two radicals. Initiation may happen spontaneously or may be induced by heat or light.

Initiation:

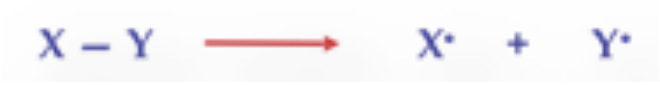

Propagation:

Termination:

Peroxides such as benzoyl peroxide,dialkyl, diaryl and acyl peroxides are common source of radical initiators. The O-O bond in peroxides is weak and reaction generally occurs at low temperatures. Some organic compounds with low-energy bonds, such as azo compounds are also used. Molecules that are cleaved by light are most often chlorine, bromine and various ketones.

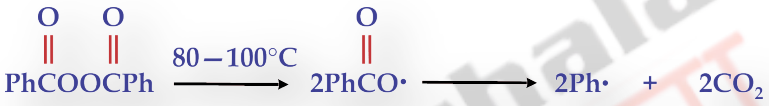

3.12 Concerted Mechanism

Concerted reaction mechanism occurs without any intermediate. The transition state involves bond breaking and bond formation. Reorganization of electrons via cyclic transition structures is the process of concerted pericyclic reactions.

Diels-Alder reaction between diene and dienophile is an example of concerted cycloaddition reaction.

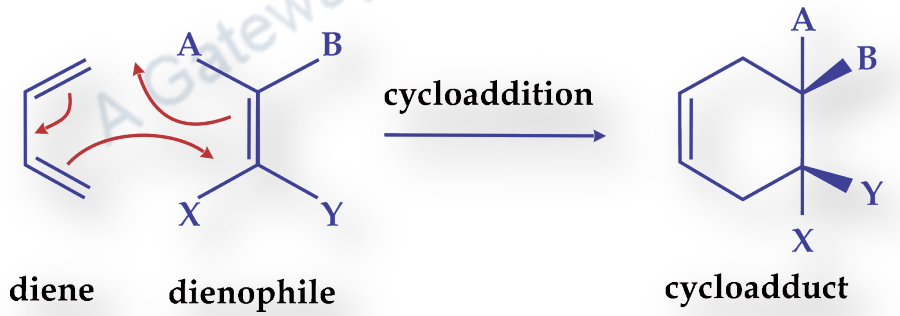

4. Summary

- Mechanism for any reaction is define as collection of number of processes that explains the overall reaction.
- The different types of mechanism via which an organic reaction may proceed are:
  - Substitution Nucleophilic Unimolecular Mechanism (S_N1)
  - Substitution Nucleophilic Bimolecular Mechanism (S_N2)
  - Substitution Nucleophilic Internal Mechanism (S_Ni)
  - Aromatic Nucleophilic Substitution Mechanism (S_NAr)
  - Substitution Radical Nucleophilic Unimolecular(SR_N1)
  - Electrophilic Aromatic Substitution Mechanism (EAS)
  - Unimolecular Elimination Mechanism (E1)
  - Bimolecular Elimination Mechanism (E2)
  - Conjugate Base Elimination Mechanism (E1cb)
  - Elimination Internal Mechanism (Ei)
  - Free Radical Mechanism
  - Concerted Mechanism

Dalton Transactions

Cite this: *Dalton Trans.*, 2011, **40**, 10007

www.rsc.org/dalton

PAPER

Chemical bonding and properties of "layered" quaternary antimonide oxide *RE*OZnSb (*RE* = La, Ce, Pr, Nd)

Kai Guo,[a,b] Zhen-Yong Man,[a] Xiao-Jun Wang,†[a] Hao-Hong Chen,[a] Mei-Bo Tang,[a] Zhi-Jun Zhang,[a] Yuri Grin[c] and Jing-Tai Zhao*[a]

Received 20th April 2011, Accepted 12th July 2011
DOI: 10.1039/c1dt10721f

An efficient route to construct a three-dimensional crystal structure is stacking of two-dimensional building blocks (2D-BBs). The crystal structures of potential thermoelectric compounds *RE*OZnSb (*RE* = La, Ce, Pr, Nd) were virtually constructed from insulating [*RE*O] and conducting [ZnSb] layers. Further optimizations performed by means of first-principles calculations show that *RE*OZnSb should exhibit semimetal or narrow band-gap semiconductor behaviors, which is a prerequisite for high thermoelectric efficiency. The analysis of the electron localizability indicator for LaOZnSb reveals mostly covalent polar interactions between all four kinds of atoms. The electron density yields completely balanced ionic-like electronic formula $La^{1.7+}O^{1.2-}Zn^{0.4+}Sb^{0.9-}$. Furthermore, the samples of *RE*OZnSb have been synthesized *via* solid-state reaction, and their crystal structures were confirmed by powder X-ray diffraction. The differences in cell parameters between the theoretically optimized and the experimental values are smaller than 2%. The temperature dependence of the magnetic susceptibility shows that LaOZnSb is diamagnetic above 40 K, whereas CeOZnSb, PrOZnSb and NdOZnSb are Curie–Weiss-type paramagnets. Electrical conductivity and Seebeck effect measurements indicate that *RE*OZnSb are p-type semiconductors. A considerably high Seebeck coefficient and low thermal conductivity were obtained for pure LaOZnSb, but its low electrical conductivity leads to a small *ZT*. The high adjustability of the crystal structure as well as properties by optimization of the chemical composition in the compounds *RE*OZnSb provide good prospects for achieving high thermoelectric efficiency.

1. Introduction

Till now, the rational design of new inorganic compounds absorbs solid-state chemists and materials scientists. Thereby serendipity plays an important role to explore new materials in spite of much time consumed.[1–3] Controlling the crystal structure and microstructure of materials is a prerequisite in order to master distinct chemical and physical properties in solids. Therefore, considerable efforts have been devoted to this field and two main approaches were proposed: computer simulation of the energy landscapes in chemical systems[4,5] and construction of new compounds of building blocks by using the concept intergrowth or structural series.[6–10] The well-known crystal structure of ZrCuSiAs can be considered as a model system for such a consideration.

The tetragonal crystal structure of ZrCuSiAs is built of [ZrSi] and [CuAs] layers stacked alternately along the *c*-axis. It has the symmetry of the space group *P*4/*nmm* and was first described by Johnson and Jeitschko as a "filled" PbFCl type.[11,12] Because of their interesting physical properties, the tetragonal layered materials containing transition elements gained a remarkable renaissance in recent years; we mention here $MCu[Q_{1-x}Q'_x]F$ (*M* = Ba, Sr; *Q*, *Q*′ = S, Se, Te),[13,14] *RE*OCu*Ch* (*RE* = trivalent rare-earth metals; *Ch* = S, Se, and Te),[15,16] and *RE*O*MPn* (*RE* = rare-earth metals; *M* = Mn, Fe, Co, and Ni *etc.*; *Pn* = P, As, Sb) *etc.*[17–22] The iron oxyarsenides were first prepared in W. Jeitschko's group;[23] later Yoichi Kamihara *et al.* found a transition from a normal to a superconducting state at 26 K in iron-based layered superconductor $La[O_{0.89}F_{0.11}]FeAs$ due to the strong interactions between the electrons confined in the FeAs layer.[19] LaOCuS has an optical band gap of 3.1 eV and exhibits p-type electrical conductivity because of the hybridization of Cu and S states.[24] The layered oxyselenide $La_{1-x}Sr_xCuOSe$ was reported as a candidate for thermoelectric material.[25]

It might be reasonable to suppose that the inter-layer and/or intra-layer atomic interactions in the compounds with this unique structure have significant influence on the novel

[a]*Key Laboratory of Transparent Opto-Functional Inorganic Materials of Chinese Academy of Sciences, Shanghai Institute of Ceramics, 1295 Ding Xi Road, Shanghai, 200050, PR China. E-mail: jtzhao@mail.sic.ac.cn; Fax: +86-21-52413122; Tel: +86-21-52412073*
[b]*Graduate School of Chinese Academy of Sciences, 19A Yu Quan Road, Beijing, 100039, PR China*
[c]*Max-Planck-Institut für Chemische Physik fester Stoffe, Nöthnitzer Str. 40, Dresden 01187, Germany*
† Current address: Laboratory of Inorganic Chemistry, ETH Zürich, Wolfgang-Pauli-Straße 10, CH-8093 Zürich, Switzerland.

properties. So, LaOCuS represents a nice model system with p-type semiconducting behavior, emerging from the wide-gap or insulating properties of oxides and narrow-gap or semiconducting properties of chalcogenides.[23] Representatives of the compounds with layered crystal structure of the $CaAl_2Ge_2$ type[26] also show distinct functionality of the layers (in the case of [ZnSb]), as in high-efficiency thermoelectric materials $Ca_xYb_{1-x}Zn_2Sb_2$[27] and $EuZn_2Sb_2$.[28] The intra-layer atomic interactions in [ZnSb] play a significant role in electronic transport and the total thermoelectric properties can be tuned by altering the intra-layer interaction as well as the layer's interaction with the embedded in-between cations. The electronic and the thermal transport properties can be adjusted as independent as possibly to achieve a high thermoelectric figure of merit ZT ($ZT = (\alpha^2\sigma/\kappa)T$, where α, σ, κ, and T are the Seebeck coefficient, electrical conductivity, total thermal conductivity, and absolute temperature, respectively).[29,30] A combination of insulating and conducting layers in the same structure might open the possibility to tune the properties in an anisotropic manner, *i.e.* maintaining good electronic transport properties in the conducting layer while achieving low thermal conductivity involving the insulating layer. This constitutes the basic needs for development of potential thermoelectric materials.

The crystal structure,[31–33] Sb Mössbauer effect,[32,34] low-temperature electrical,[33] optical[34] and magnetic properties[35] have been already studied for selected compounds *RE*OZnSb (*RE* = La–Nd, Sm). However, taking into account the above considerations, an understanding of the chemical bonding in the sense of the intergrowth concept and its relationship to the thermoelectric properties may build a new strategy in design of new thermoelectrics. In this report we present the chemical bonding, crystal structure and thermoelectrically relevant properties of quaternary antimonide oxide *RE*OZnSb (*RE* = La, Ce, Pr, Nd).

2. Experimental section

2.1. Preparation of samples

The compounds were synthesized *via* solid-state reactions. Rare earth metals (La, Ce, Pr, Nd, purity 99.9%), oxides (La_2O_3, CeO_2, Pr_6O_{11}, Nd_2O_3, purity 99.999%), Zn metal (purity 99.999%), and Sb metal (purity 99.999%) were used as starting materials. Stoichiometric amounts of constituents (ratio of *RE* : O : Zn : Sb = 1 : 1 : 1 : 1) were put in graphite crucibles in a N_2-filled glove box (H_2O/O_2 levels below 0.1 ppm), then the crucibles were sealed in evacuated silica tubes and heated up to 1173 K for 3 days with a rate of 2 K min^{-1}. In order to make the solid reaction complete and increase the homogeneity of the products, the resulting products were ground to fine powders and pressed into pellets. The pellets were sintered at 1173 K in an evacuated quartz tube and maintained for 2 days for the second stage of the solid-state reaction. The as-synthesized black-colored samples after cooling down to room temperature were kept in a glove box to prevent oxidation. The bulk material for measuring thermoelectric properties was prepared using LaOZnSb powder by Spark Plasma Sintering (Dr Sinter SPS 2040 setup manufactured by Sythex SPS, Tokyo) at 903 K for 5 min under uniaxial pressure of 70 MPa in a vacuum.

2.2. Characterization

X-Ray powder diffraction (XRPD) data of the samples *RE*OZnSb at ambient temperature were collected on a Rigaku D/Max-2200 PC diffractometer at 40 kV and 40 mA (Cu $K_{\alpha 1}$ radiation, λ = 1.54056 Å, 2θ range from 10° to 100° with a step size of 0.02°). The atomic parameters of ZrCuSiAs were taken as starting values and the crystal structures of LaOZnSb were refined using WinCSD software[36] (full-profile Rietveld refinement) with anisotropic atomic displacement parameters for La, Zn, Sb, and an isotropic displacement parameter for the O. Seebeck coefficient and electrical conductivity measurements were done under an argon atmosphere using an ULVAC-RIKO ZEM-3 system on prism-shaped samples. The thermal conductivity was obtained from the thermal diffusivity and the specific heat measured by the laser flash technique (LFA 447, Netzsch). Magnetization measurements (field cooling) were performed with a physical property measurement system (PPMS) at applied fields (H) up to 5 T.

2.3. Electronic structure calculations and analysis of chemical bonding

First-principles calculations of the band structure were performed using the Castep code, which utilizes pseudopotentials to describe electron–ion interactions and represents electronic wave functions by means of a plane-wave basis set.[37] Generalized gradient approximation was applied to model the exchange–correlation energy as formulated by Perdew, Burke and Ernzerhof.[38,39] The unit cell parameters and atomic positional parameters were optimized applying ultra-soft pseudopotentials with a cutoff energy of 600 eV. Monkhorst–Pack meshes of (6 × 6 × 3) were used for the integration in the Brillouin zone. The following states are treated as valence states: La ($5s^25p^65d^16s^2$), Ce ($4f^15s^25p^65d^16s^2$) Pr ($4f^35s^25p^66s^2$), Nd ($4f^35s^25p^65d^16s^2$), O ($2s^22p^4$), Zn ($3d^{10}4s^2$) and Sb ($5s^25p^3$). The residual forces and energy convergence tolerance were smaller than 0.01 eV $Å^{-1}$ and 1.0×10^{-6} eV $atom^{-1}$ at the end of calculations.

Analysis of chemical bonding was carried out for LaOZnSb using the TB-LMTO-ASA program package.[40] The Barth–Hedin exchange potential[41] was employed for the LDA calculations. The radial scalar-relativistic Dirac equation was solved to get the partial waves. Because the calculation within the atomic sphere approximation (ASA) includes corrections for the neglect of interstitial regions and partial waves of higher order,[42] an addition of empty spheres was not necessary. The following radii of the atomic spheres were applied for the calculations: r(La) = 1.802 Å, r(Zn) = 1.653 Å, r(Sb) = 1.953 Å, r(O) = 1.149 Å. A basis set containing La(6s, 5d, 4f), Zn(4s, 4p, 3d), Sb(5s, 5p) and O(2p) orbitals was employed for a self-consistent calculation with La(6p), Sb(5d, 4f) and O(3s, 3d) functions being downfolded. The electron localizability indicator (ELI, Υ)[43] was evaluated in the ELI-D representation according to ref. 44 and 45 with an ELI-D module within the TB–LMTO–ASA program package.[40] ELI-D and electron density were analyzed using the program Basin[46] with consecutive integration of the electron density in basins, which are bound by zero-flux surfaces in the ELI-D or electron density gradient field with a procedure proposed by R. F. W. Bader for the electron density.[47]

3. Results and discussion

3.1. Construction and optimization of the crystal structures of *RE*OZnSb

Within the intergrowth concept, the crystal structures of *RE*OZnSb can be described by stacking of [*RE*O] layers from *RE*OCl and [ZnSb] layers from NaZnSb along the tetragonal *c*-axis, as shown in Fig. 1. Zinc is surrounded by four antimony atoms forming edge-sharing tetrahedrons [$ZnSb_{4/4}$], which are interconnected to produce a [ZnSb] layer. Similarly, a [LaO] layer is formed by edge-sharing tetrahedrons [$OLa_{4/4}$]. The [LaO] layer is supposed to be insulating, while the [ZnSb] layer should serve as a carrier conduction path. Assuming the best possible match of the layers, the lattice parameter a_0 can be determined as the average value of a(*RE*OCl) and a(NaZnSb). In this way, the following initial lattice parameters were obtained: $a_0 = 4.2781$ Å for LaOZnSb, $a_0 = 4.2633$ Å for CeOZnSb, $a_0 = 4.2465$ Å for PrOZnSb and $a_0 = 4.2400$ Å for NdOZnSb. Utilizing the parameters a_0 and the interatomic distances from the database,[48] approximate values of the c_0 parameters, atomic coordinates z_{RE} and z_{Sb} were calculated according to the following equations:[2]

$$c_0 = 2\times\left(\sqrt{d_{RE-O}^2 - \frac{1}{4}a_0^2} + \sqrt{d_{RE-Sb}^2 - \frac{1}{2}a_0^2} + \sqrt{d_{Zn-Sb}^2 - \frac{1}{4}a_0^2}\right) \quad (1)$$

$$z_{RE} = \sqrt{d_{RE-O}^2 - \frac{1}{4}a_0^2} \Big/ c_0 \quad (2)$$

$$z_{Sb} = 0.5 + \sqrt{d_{Zn-Sb}^2 - \frac{1}{4}a_0^2} \Big/ c_0 \quad (3)$$

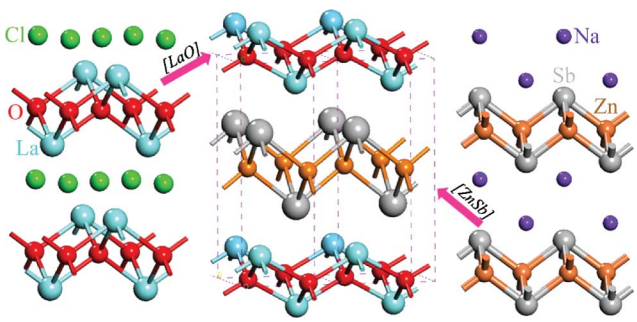

Fig. 1 The LaOZnSb crystal structure (middle) as a stacking of the [LaO] layers from LaOCl (left) and [ZnSb] layers from NaZnSb (right).

All parameters of the geometrically predicted structures are listed in Table 1. The cell parameters a_0 and c_0 decrease with the decreasing ionic radii of the rare-earth elements. Optimizations of the crystal structures were carried out through first-principles calculations and the energy convergence indicated the thermodynamical stability of the compounds in agreement with the experimental results. The optimized parameters and experimentally obtained values are summarized in Table 1 too. The differences between the optimized and experimentally found lattice parameters are within 2%, which is within the usual range by this kind of optimization of the crystal structures.[49,50] Close agreement between the experimental and theoretically optimized structural parameters allowed the use of the latter for the further analysis of the ground-state properties.

3.2. Electronic structure of *RE*OZnSb compounds

Electronic structure and density of states (DOS) were calculated on the basis of relaxed structures, as shown in Fig. 2. On the basis of these calculations, semiconducting or semimetallic behavior was predicted for all four compounds *RE*OZnSb, as is necessary for an efficient thermoelectric material. It should be mentioned that the value of the band gap is usually underestimated due to the well-known DFT reason using GGA as the exchange–correlation potential.[51] Therefore, the experimental gap is expected to be larger than the calculated one. Fig. 3 shows the total density of states and partial density of states of LaOZnSb in the energy range between −35 eV to 7 eV, where five ranges can be recognized. With the energy below −30 eV, the DOS is dominated by La 6s states. The bonding band from −20 eV to −14 eV is mainly formed by La 5p and O 2s states, indicating considerable covalent interactions between La and O. Mainly Sb 5s and Zn 3d states are located in the range of −11 eV to −6 eV and may also hybridize. It is worth noting that both of the valence and conduction band widths extend 6 eV.

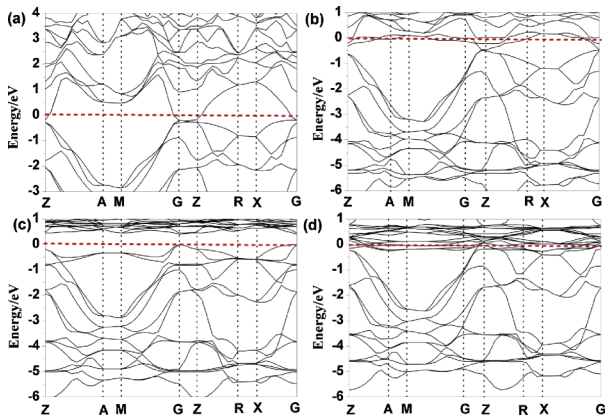

Fig. 2 Band structures of *RE*OZnSb: (a) *RE* = La; (b) *RE* = Ce; (c) *RE* = Pr; (d) *RE* = Nd.

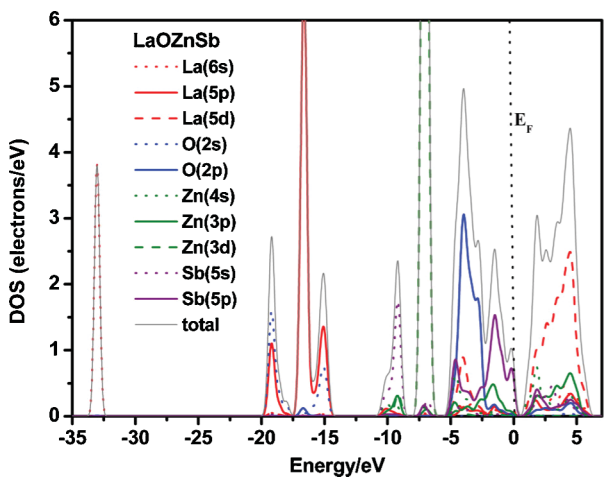

Fig. 3 Total electronic DOS of LaOZnSb with partial contributions of selected states.

Table 1 The geometrically deduced, theoretically optimized and experimental unit cell parameters of *RE*OZnSb[c]

		LaOZnSb	CeOZnSb	PrOZnSb	NdOZnSb
a_0/Å	Geometrically deduced	4.278	4.263	4.247	4.240
	Optimized	4.263	4.190	4.146	4.170
	Experimental	4.229(5)[a]	4.202(4)[a]	4.183(1)[a]	4.163(6)[a]
		4.2267(6)[32]	4.1976(4)[31]	4.1763(4)[31]	4.159(1)[32]
Differences[b]		−0.78%	0.29%	0.87%	−0.14%
c_0/Å	Geometrically deduced	8.553	8.246	8.299	8.097
	Optimized	9.750	9.530	9.598	9.594
	Experimental	9.552(2)[a]	9.494(8)[a]	9.462(3)[a]	9.456(2)[a]
		9.538(2)[32]	9.474(1)[31]	9.451(1)[31]	9.454(4)[32]
Differences[b]		−2.0%	−0.38%	−1.44%	−1.46%
RE(1/4 1/4 *z*) *z* =	Geometrically deduced	0.1229	0.1252	0.1262	0.1212
	Optimized	0.1235	0.1217	0.1184	0.1135
Sb(3/4 3/4 *z*) *z* =	Geometrically deduced	0.7056	0.7144	0.7142	0.7200
	Optimized	0.6767	0.6852	0.6858	0.6853

[a] This work [b] Differences are calculated as $(a_0(\text{Opt.}) - a_0(\text{Exp.}))/a_0(\text{Exp.})$ and $(c_0(\text{Opt.}) - c_0(\text{Exp.}))/c_0(\text{Exp.})$. [c] The coordinates of O and Zn are ($x_O = x_{Zn} = 0.75$, $y_O = y_{Zn} = 0.25$, $z_O = 0$, $z_{Zn} = 0.5$).

The valence band below the Fermi level is mainly composed of Sb 5s, Sb 5p and Zn 4s, Zn 3p states. The conduction band above the Fermi level is dominated by Zn 4s, Zn 3p, Sb 5p and La 5d states. Therefore, the transport behaviors of the compounds *RE*OZnSb may be different since the diffuse Zn-4s orbitals slightly hybridize with the 5d- and 4f-orbitals of the rare earth element and thus the energy is altered.[52]

3.3. Chemical bonding in compounds *RE*OZnSb

The chemical bonding pattern in LaOZnSb was further evaluated by the analysis of the electron localizability indicator in combination with the electron density. The evaluation of the electron density according to the QTAIM method of Bader[47] yielded an atomic basin for each atom. The shapes of the basins for La, Zn, Sb and O are shown in Fig. 4. Integration of the electron density within the atomic basins gives 9.2 electrons for oxygen ($O^{1.2-}$), 50.9 electrons for antimony ($Sb^{0.9-}$), 29.6 electrons for zinc ($Zn^{0.4+}$), and 55.3 electrons for lanthanum ($La^{1.7+}$), yielding the completely balanced electronic formula $La^{1.7+}O^{1.2-}Zn^{0.4+}Sb^{0.9-}$. QTAIM charges and the charge transfer are in agreement with the electronegativity relationships between the components: EN(La) < EN(Zn) < EN(Sb) < EN(O). The absolute values of the atomic charges are smaller than those expected from the usual oxidation states (+3 for La, −2 for O, +2 for Zn and −3 for Sb). This indicates reduced ionicity and partial covalency of the atomic interactions in the crystal structure.

The bonding situation was analyzed in detail by means of the electron localizability indicator in the ELI-D representation (Fig. 5). In the case of lanthanum, the sixth shell is completely absent. These electrons are transferred to the neighboring atoms. Charge transfer causes ionic interaction of the lanthanum with its environment. In addition, the distribution of ELI-D in the penultimate (fifth) shell is strongly deviating from the spherical one, which is characteristic for the non-interacting atoms. This deviation is quantified by the structuring index ε (the difference

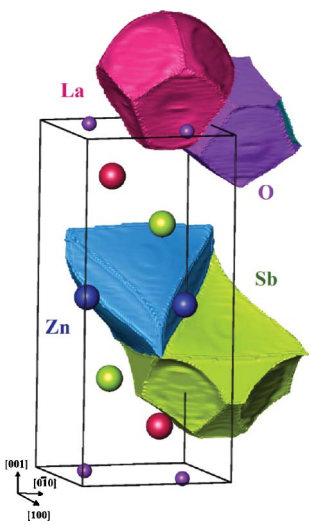

Fig. 4 The shape of the QTAIM atomic volumes in LaOZnSb. The according charges are 9.2 e^- for oxygen ($O^{1.2-}$), 50.9 e^- for antimony ($Sb^{0.9-}$), 29.6 e^- for zinc ($Zn^{0.4+}$), and 55.3 e^- for lanthanum ($La^{1.7+}$), yielding completely balanced formula $La^{1.7+}O^{1.2-}Zn^{0.4+}Sb^{0.9-}$.

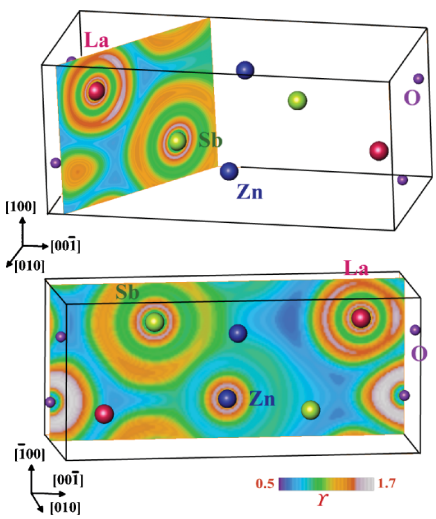

Fig. 5 Electron localizability indicator in LaOZnSb. Structuring of the outer shells of Sb and O as well as the penultimate (fifth) shell for La reveals their participation in the bonding. The structuring of the fourth shell of Zn is only weakly recognizable.

between the highest ELI-D value in the examined shell and the ELI-D value at which the localization domain is without a 'hole').[53] For lanthanum it is 0.122, which is remarkably large for an *RE* cation. Formation of 'holes' in the penultimate shell of lanthanum in the direction of the neighboring oxygen atoms and a deformation of the second shell of oxygen is a signature of the (polar) covalent bonds between them. These bonds are mainly contributing to the formation of the [LaO] layers.

The formation of the [ZnSb] layers is less pronounced from the point of view of chemical bonding. The most interesting is the interaction between the zinc and the antimony: there are no dedicated maxima on the Zn–Sb lines, which are usually expected for a covalent interaction caused by a small electronegativity difference. Only in the structuring of the valence shell of Sb the covalent character of this interaction may be recognized. At the same time, a local enhancement of the ELI values is observed in the third shell of zinc, toward lanthanum, indicating also a significant covalent (polar) interaction. In addition, the valence shell of antimony (fifth) is also strongly structured. Here, already local maxima are formed close to the lines to the neighboring oxygen and lanthanum atoms from the neighboring [LaO] layer revealing the (polar) covalent inter-layer interaction. Antimony behaves here as an electron donor toward oxygen and an acceptor toward the lanthanum atoms. Thus, analysis of the atomic interactions does not reveal clear separation between the [LaO] and [ZnSb] layers from the point of view of chemical bonding. This should have consequences on the bonding-relevant transport properties, *i.e.* reducing the thermal transport.

3.4. Syntheses, crystal structure and materials morphology of *RE*OZnSb

The X-ray diffraction patterns of as-synthesized *RE*OZnSb samples are shown in Fig. 6. They match very well the simulated pattern of optimized structures, indicating that the samples are composed mainly of one phase, and only traces of ZnSb as impurity were detected. The patterns were indexed with a tetragonal lattice (space group *P*4/*nmm*). With the atomic radii decreasing (from La to Nd), the diffraction peaks shift to the higher angles systematically. The unit cell parameters indexed and

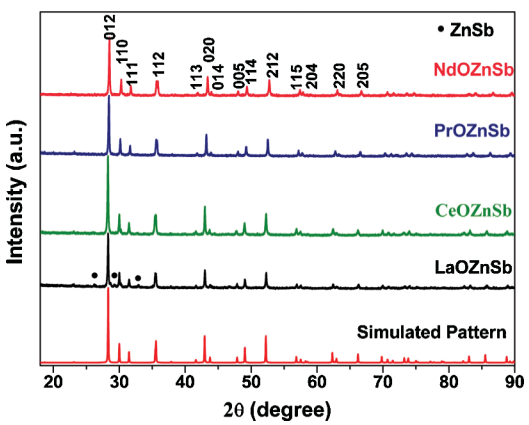

Fig. 6 Calculated X-ray diffraction pattern for the optimized model of the crystal structure of LaOZnSb in comparison with experimental patterns of *RE*OZnSb compounds prepared by solid-state reactions. Reflections of the impurity phase ZnSb are marked.

Table 2 Experimental atomic coordinates and displacement parameters (pm^2) for LaOZnSb. U_{eq} is defined as one third of the trace of the orthogonalized U_{ij} tensor. $U_{12} = U_{13} = U_{23} = 0$

Atom	W. site	x	y	z	$U_{11} = U_{22}$	U_{33}	U_{eq}
La	2*c*	1/4	1/4	0.12050(8)	60(3)	82(4)	67(2)
Zn	2*b*	3/4	1/4	1/2	120(5)	131(9)	124(4)
Sb	2*c*	1/4	1/4	0.68011(8)	84(3)	99(4)	89(2)
O	2*a*	3/4	1/4	0			70(20)[a]

[a] Isotropic displacement parameters for O.

Table 3 Interatomic distances (pm) for LaOZnSb

La	4	O	240.79(4)	Sb	4	Zn	272.59(5)
	4	Sb	354.58(6)		4	La	354.58(6)
Zn	4	Sb	272.59(5)	O	4	La	240.79(4)

refined from the XRD patterns are summarized in Table 1 and are in agreement with the theoretical results with the differences smaller than 2%. The X-ray powder pattern for LaOZnSb is shown in Fig. 7. The parameters $a_0 = 4.23079(1)$ Å and $c_0 = 9.54560(6)$ Å are obtained by the Rietveld technique. The atomic positional and displacement parameters were refined and are listed in Tables 2 and 3. Furthermore, the distances between [*RE*O] and [ZnSb] are all larger than 1.84 Å ($(z_{RE} - z_{Sb}) \times c_0$) obtained from optimization results. Thus, it is expected that this natural 'superlattice' may scatter phonons, thus reducing the thermal conductivity.

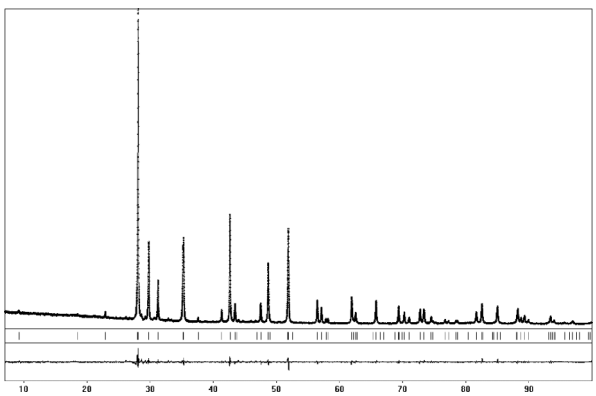

Fig. 7 Rietveld refinement result for LaOZnSb. The continuous profile and dots represent the calculated XRD intensity and experimental data, respectively. The bottom profile is the difference between the experimental and calculated intensities ($R_{wp} = 8.18\%$, $R_B = 4.97\%$).

3.5. Physical properties of *RE*OZnSb

The temperature dependence of the molar magnetic susceptibility of polycrystalline samples *RE*OZnSb is presented in Fig. 8. The measurements reveal diamagnetism above 40 K for LaOZnSb. In contrary, CeOZnSb, PrOZnSb and NdOZnSb are paramagnetic. The temperature dependencies follow the Curie–Weiss law $\chi(T) = C/(T - \theta)$, where χ is the molar magnetic susceptibility, $C = N_A\mu_{eff}^2/3\kappa_B$ is the Curie constant, and θ is the Weiss temperature. A linear fit of the inverse magnetic susceptibility as a function of the temperature is employed (Fig. 8(b)), yielding effective paramagnetic moments μ of 2.44 μ_B, 3.41 μ_B and 3.21 μ_B characteristic for the trivalent Ce ($4f^1$), Pr ($4f^2$) and Nd ($4f^3$)

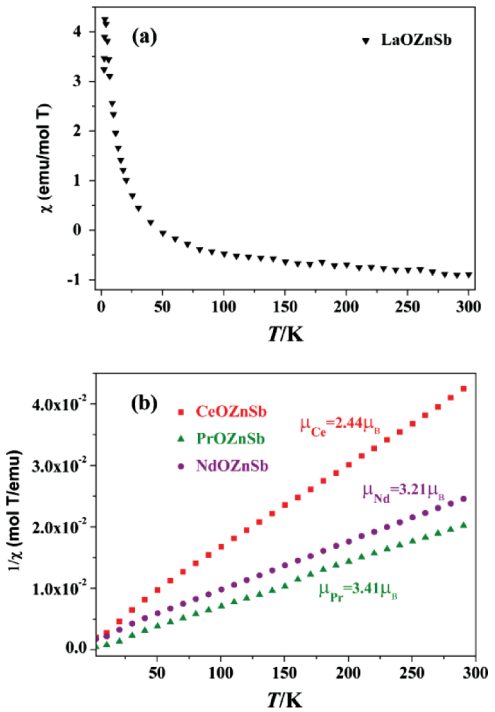

Fig. 8 Magnetic susceptibility *vs.* temperature for LaOZnSb (a) and the inverse magnetic susceptibility *vs.* temperature for CeOZnSb, PrOZnSb and NdOZnSb (b). Data are collected in a field-cooling mode ($H = 5$ T).

ions, respectively (*cf.* theoretical values of the magnetic moments $\mu_{Ce3+} = 2.54\ \mu_B$, $\mu_{Pr3+} = 3.5\ \mu_B$ and $\mu_{Nd3+} = 3.5\ \mu_B$).

The temperature dependencies of the electrical conductivity and Seebeck coefficient for LaOZnSb are shown in Fig. 9 (a) and (b). With increasing temperature from 300 K to 665 K, the Seebeck coefficient decreases from +206 μV K^{-1} to +160 μV K^{-1}, suggesting a p-type conductivity. On the contrary, the electrical conductivity monotonously increases from 6.0×10^2 S m^{-1} to 1.9×10^3 S m^{-1}, originated from more carriers excited at elevated temperature. During the activation temperature of intrinsic carriers, the band gap can be extracted from the carrier activation-dominated electrical conductivity. As can be seen in Fig. 9 (a) insert, a $\ln(\sigma/\sigma_0)$–$1000/T$ plot was carried out to obtain the band gap. On the basis of the slope coefficient calculated from the curve, the value of 0.3 eV was determined. The room-temperature electrical conductivity of LaOZnSb is larger than that of the isomorphic compounds LaOZnP and LaOZnAs because of a smaller value of the band gap (LaOZnP ≈ 1.7 eV; LaOZnAs ≈ 1.5 eV).[54,55] In comparison with another related compound $La_{0.95}Sr_{0.05}CuOSe$[24] and $FeSb_2$,[56] LaOZnSb exhibits high electrical conductivity and a large Seebeck coefficient above room-temperature, thus large power factors ($\alpha^2\sigma$). The thermal conductivities are all well below 1.5 W m^{-1} K^{-1} (Fig. 9 (c)), revealing a targeted low thermal conductivity. Thus, the experimental results are in good agreement with the above discussed theoretical calculations. The thermoelectric figure of merit ZT for LaOZnSb increases with increasing temperature from 0.005 at 311 K to 0.032 at 665 K and may reach higher above 665 K from the trend of the curve. Although a considerably high Seebeck coefficient and low thermal conductivity were obtained for LaOZnSb, its low electrical conductivity leads to a small ZT.

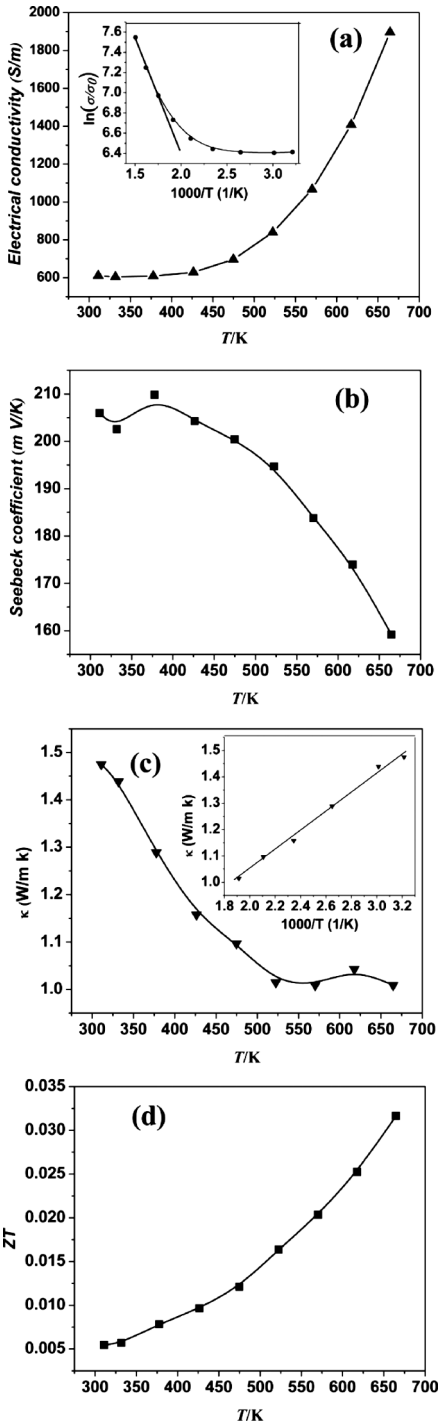

Fig. 9 Temperature dependences of (a) electrical conductivity, (b) Seebeck coefficient, (c) thermal conductivity and (d) thermoelectric figure of merit ZT for LaOZnSb.

4. Conclusions

The structural models of the compounds *RE*OZnSb (*RE* = La, Ce, Pr, Nd, ZrCuSiAs-type) obtained from the intergrowth concept were optimized by first-principle calculations. Analysis of chemical bonding in the optimized LaOZnSb revealed polar covalent interaction between La and O, and between Zn and Sb. In addition, inter-layer covalent interactions between Sb and La and O are

detected. Band structure and electronic DOS calculations on the optimized structure models predicted narrow-gap semiconducting behavior for all four compounds *RE*OZnSb (*RE* = La, Ce, Pr, Nd). The predicted crystal structures and physical behaviors were confirmed by the samples synthesized by solid-state reactions. The experimental unit cell parameters were in agreement with the optimized values within 2%. The relatively small thermoelectric figure of merit value *ZT* for pure LaOZnSb resulted from a considerably high Seebeck coefficient, low thermal conductivity and low electrical conductivity. Similar results but with higher electrical conductivity might be expected for the compounds of the other rare earth elements. The high adjustability of the structures as well as transport properties by substitution/doping different elements at different atomic sites in these compounds provide good opportunity for improving thermoelectric properties. Further work at optimizing thermoelectric properties in these compounds is being done in our lab.

Acknowledgements

We would like to acknowledge the financial support by the National Basic Research Program of China under Project No. 2007CB607503, National Natural Science Foundation of China under Project No. 0821004, and the MPG-CAS Partner Group Program.

Notes and references

1 L. Cario, H. Kabbour and A. Meerschaut, *Chem. Mater.*, 2005, **17**, 234.
2 H. Kabbour, L. Cario and F. Boucher, *J. Mater. Chem.*, 2005, **15**, 3525.
3 H. Kabbour, L. Cario, M. Danot and A. Meerschaut, *Inorg. Chem.*, 2006, **45**, 917.
4 J. C. Schön and M. Jansen, *Z. Kristallogr.*, 2001, **216**, 307.
5 M. Jansen, *Angew. Chem., Int. Ed.*, 2002, **41**, 3746.
6 Yu. N. Grin, Ya. P. Yarmolyuk and E. I. Gladyshevskii, *Sov. Phys. Crystallogr.*, 1982, **27**, 413.
7 E. Parthé, B. A. Chabot and K. Cenzual, *Chimia*, 1985, **39**, 164.
8 G. Férey, *J. Solid State Chem.*, 2000, **152**, 37.
9 C. Mellot-Draznieks, S. Girard, G. Férey, J. C. Schon, Z. Cancarevic and M. Jansen, *Chem.–Eur. J.*, 2002, **8**, 4102.
10 O. M. Yaghi, M. O'Keefe, N. W. Ockwig, H. K. Chae, M. Eddaoudi and J. Kim, *Nature*, 2003, **423**, 705.
11 V. Johnson and W. Jeitschko, *J. Solid State Chem.*, 1974, **11**, 161.
12 R. Pöttgen and D. Johrendt, *Z. Naturforsch.*, 2008, **63b**, 1135.
13 C. H. Park, D. A. Keszler, H. Yanagi and J. Tate, *Thin Solid Films*, 2003, **445**, 288.
14 H. Yanagi, J. Tate, S. Park, C. H. Park and D. A. Keszler, *Appl. Phys. Lett.*, 2003, **82**, 2814.
15 S. I. Inoue, K. Ueda and H. Hosono, *Phys. Rev. B*, 2001, **64**, 245211.
16 K. Ueda, K. Takafuji, H. Hiramatsu, H. Ohta, T. Kamiya, M. Hirano and H. Hosono, *Chem. Mater.*, 2003, **15**, 3692.
17 Y. Kamihara, H. Hiramatsu, M. Hirano, R. Kawamura, H. Yanagi, T. Kamiya and H. Hosono, *J. Am. Chem. Soc.*, 2006, **128**, 10012.
18 T. Watanabe, H. Yanagi, T. Kamiya, Y. Kamihara, H. Hiramatsu, M. Hirano and H. Hosono, *Inorg. Chem.*, 2007, **46**, 7719.
19 Y. Kamihara, T. Watanabe, M. Hirano and H. Hosono, *J. Am. Chem. Soc.*, 2008, **130**, 3296.
20 X. H. Chen, T. Wu, G. Wu, R. H. Liu, H. Chen and D. F. Fang, *Nature*, 2008, **453**, 761.
21 H. H. Wen, *Adv. Mater.*, 2008, **20**, 3764.
22 B. I. Zimmer, W. Jeitschko, J. H. Albering, R. Glaum and M. Reehuis, *J. Alloys Compd.*, 1995, **229**, 238.
23 P. Quebe, L. J. Terbüchte and W. Jeitschko, *J. Alloys Compd.*, 2000, **302**, 70.
24 K. Ueda, H. Hiramatsu, M. Hirano, T. Kamiya and H. Hosono, *Thin Solid Films*, 2006, **496**, 8.
25 M. Yasukawa, K. Ueda and H. Hosono, *J. Appl. Phys.*, 2004, **95**, 3594.
26 F. Gascoin, S. Ottensmann, D. Stark, S. M. Haile and G. J. Snyder, *Adv. Funct. Mater.*, 2005, **15**, 1860.
27 X. J. Wang, M. B. Tang, J. T. Zhao, H. H. Chen and X. X. Yang, *Appl. Phys. Lett.*, 2007, **90**, 232107.
28 H. Zhang, J. T. Zhao, Yu. Grin, X. J. Wang, M. B. Tang, Z. Y. Man, H. H. Chen and X. X. Yang, *J. Chem. Phys.*, 2008, **129**, 164713.
29 G. K. H. Madsen, *J. Am. Chem. Soc.*, 2006, **128**, 12140.
30 B. Poudel, Q. Hao, Y. Ma, Y. C. Lan, A. Minnich, B. Yu, X. Yan, D. Z. Wang, A. Muto, D. Vashaee, X. Y. Chen, J. M. Liu, M. S. Dresselhaus, G. Chen and Z. Ren, *Science*, 2008, **320**, 634.
31 P. Wollesen, J. W. Kaiser and W. Jeitschko, *Z. Naturforsch.*, 1997, **52b**, 1467.
32 I. Schellenberg, T. Nilges and R. Pöttgen, *Z. Naturforsch.*, 2008, **63b**, 834.
33 Y. Takano, S. Komatsuzaki, H. Komasaki, T. Watanabe, Y. Takahashi and K. Takase, *J. Alloys Compd.*, 2008, **451**, 467.
34 I. Schellenberg, H. Lincke, W. Hermes, V. Dittrich, R. Glaum, M. H. Möller and R. Pöttgen, *Z. Naturforsch.*, 2010, **65b**, 1.
35 S. Komatsuzaki, Y. Ohki, M. Sasaki, Y. Takahashi, K. Takase, Y. Takano, K. Sekizawa, *Low Temperature Physics, Pts A and B*, ed. Y. Takano, S. P. Hershfield, P. J. Hirschfeld and A. M. Goldman, Amer. Inst. Physics, Melville, 2006, **850**, 1255.
36 L. G. Akselrud, P. Yu. Zavalii, Yu. Grin, V. K. Pecharsky, B. Baumgartner and E. Wölfel, *Mater. Sci. Forum*, 1993, **335**, 133.
37 S. J. Clark, M. D. Segall, C. J. Pickard, P. J. Hasnip, M. J. Probert, K. Refson and M. C. Payne, *Z. Kristallogr.*, 2005, **220**, 567.
38 J. P. Perdew, K. Burke and M. Ernzerhof, *Phys. Rev. Lett.*, 1996, **77**, 3865.
39 J. P. Perdew, K. Burke and M. Ernzerhof, *Phys. Rev. Lett.*, 1997, **78**, 1396.
40 O. Jepsen, A. Burkhardt and O. K. Andersen, *The Program TB-LMTO-ASA. Version 4.7*, Max-Planck-Institut für Festkörperforschung, Stuttgart, 1999.
41 U. von Barth and L. Hedin, *J. Phys.*, 1972, **C5**, 1629.
42 O. K. Andersen, *Phys. Rev.*, 1975, **B12**, 3060.
43 M. Kohout, *Int. J. Quantum Chem.*, 2004, **97**, 651.
44 M. Kohout, F. R. Wagner and Yu. Grin, *Int. J. Quantum Chem.*, 2006, **106**, 1499.
45 M. Kohout, *Faraday Discuss.*, 2007, **135**, 43.
46 M. Kohout, *Basin, Version 4.3*, 2008.
47 R. F. W. Bader, *Atoms in Molecules: A Quantum Theory*, Oxford University Press, Oxford, 1999.
48 ICSD (2010). ICSD is available at FIZ Karlsruhe at http://www.fiz-karlsruhe.de/icsd.html. ICSD now contains 132 526 crystal structures.
49 A. Mokhtari and H. Akbarzadeh, *Phys. B*, 2003, **337**, 122.
50 C. Yu, J. Liu, H. Lu, P. Li and J. Chen, *Intermetallics*, 2007, **15**, 1471.
51 G. Mallia and N. M. Harrison, *Phys. Rev. B*, 2007, **75**, 165201.
52 H. Lincke, R. Glaum, V. Dittrich, M. Tegel, D. Johrendt, W. Hermes, M. H. Möller, T. Nilges and R. Pöttgen, *Z. Anorg. Allg. Chem.*, 2008, **634**, 1339.
53 F. R. Wagner, V. Bezugly, M. Kohout and Yu. Grin, *Chem.–Eur. J.*, 2007, **13**, 5724.
54 K. Kayanuma, R. Kawamura, H. Hiramatsu, H. Yanagi, M. Hirano, T. Kamiya and H. Hosono, *Thin Solid Films*, 2008, **516**, 5800.
55 K. Kayanuma, H. Hiramatsu, M. Hirano, R. Kawamura, H. Yanagi, T. Kamiya and H. Hosono, *Phys. Rev. B*, 2007, **76**, 195325.
56 P. Sun, N. Oeschler, S. Johnsen, B. B. Iversen and F. Steglich, *J. Phys.: Conf. Ser.*, 2009, **150**, 012049.